Quarterly Progress Report

High Temperature Electrochemical Polishing of H_2S from Coal Gasification Process Streams

Grant DE-FG22-94-PC94207

July 1, 1996 - September 30, 1996

by

Professor Jack Winnick

Georgia Institute of Technology

School of Chemical Engineering

Atlanta, GA 30332-0100

DISCLAIMER

Project Objectives

Coal may be used to generate electrical energy by any of several processes, most of which involve combustion or gasification. Combustion in a coal-fired boiler and power generation using a steam-cycle is the conventional conversion method; however total energy conversion efficiencies for this type of process are only slightly over 30%[1]. Integration of a gas-cycle in the process (combined cycle) may increase the total conversion efficiency to 40%[1]. Conversion processes based on gasification offer efficiencies above 50%[1].

H_2S is the predominant gaseous contaminant in raw coal gas. Coal depending on the type and area of extraction can contain up to 5 wt% sulfur, which is converted to gaseous H_2S during gasification. Problems arise due to the corrosive nature of H_2S on metal components contained in these cycles. Because of this, H_2S concentrations must be reduced to low levels corresponding to certain power applications. For example, an integrated coal gasification-combined cycle (IGCC) process producing electricity from coal at nearly 50% overall efficiency[1] incorporates gas turbines that cannot tolerate H_2S levels above 100 ppm. Coal gasification/Molten Carbonate Fuel-Cell(MCFC) systems, achieving conversion efficiencies around 60%[2], function properly only if H_2S is below 1 ppm.

An advanced process for the separation of hydrogen sulfide (H_2S) from coal gasification product streams through an electrochemical membrane is being developed using funds from this grant. H_2S is removed from the syn-gas stream, split into hydrogen, which enriches the exiting syn-gas, and sulfur, which is condensed from an inert sweep gas stream, Figure 1. The process allows removal of H_2S without cooling the gas stream and with negligible pressure loss through the separator. The process is made economically attractive by the lack of need for a Claus process for sulfur recovery. To this extent the project presents a novel concept for improving utilization of coal for more efficient power generation.

Past experiments using this concept dealt with identifying removal of 1-2% H_2S from gases containing only H_2S in N_2[3], simulated natural gas[4,5], and simulated coal gas[6]. Data

obtained from these experiments resulted in extended studies into electrode kinetics and electrode stability in molten melts[7,8,9]. The most recent experiments evaluated the polishing application (removal of H_2S below 10 ppm) using the Electrochemical Membrane Separator (EMS). H_2S removal efficiencies over 90% were achieved at these stringent conditions of low H_2S concentrations proving the technologies polishing capabilities.

Other goals include optimization of cell materials capable of improving cell performance. Once cell materials are defined, cell experiments determining maximum removal capabilities and current efficiencies will be conducted.

Also, a model theoretically describing the preferred reduction of H_2S, the transport of S^{2-}, and the competing transport of CO_2 will be investigated. The model should identify the maximum current efficiency for H_2S removal, depending on variables such as flow rate, temperature, current application, and the total cell potential.

Introduction

The Electrochemical Membrane Separator (E.M.S.), the focus of experimental work, purges a fuel gas contaminated with H_2S. This is done by reducing the most electro-active species in the gas stream. In this case, H_2S is reduced by the following:

$$H_2S + 2e^- \rightarrow H_2 + S^{2-} \qquad (1)$$

A membrane which contains sulfide ions in a molten salt electrolyte will act to transport the ions across to the anode. If the membrane is impermeable to H_2 diffusion from the cathode side, an inert sweep gas can be used to carry the vaporous oxidized sulfur downstream to be condensed.

$$S^{2-} \rightarrow 1/2\, S_2 + 2e^- \qquad (2)$$

Processes to remove H_2S typically rely on low-to -ambient temperature adsorption, followed by sorbent regeneration and Claus plant treatment for conversion of H_2S to a salable by-product, sulfur. Although effective, this type of removal is very process-intensive as well as energy-inefficient due to low temperature operation. Gasification streams generally range from 500°C - 1000°C, requiring cooling before and reheating after process gas sweetening. Although these technologies have proven capable of meeting H_2S levels required by MCFC, there are several disadvantages inherent to these processes[10,11].

Alternative high temperature methods are presently available, but process drawbacks including morphological changes in catalytic beds[12] or inefficient molten salt sorbent processes[13] negate savings incurred through energy efficient removal temperatures.

An electrochemical membrane separation system for removing H_2S from coal gasification product streams is the subject of this investigation. The high operating temperature, flow-through design, and capability of selective H_2S removal and direct production of elemental

sulfur offered by this process provide several advantages over existing and developmental H_2S removal technologies.

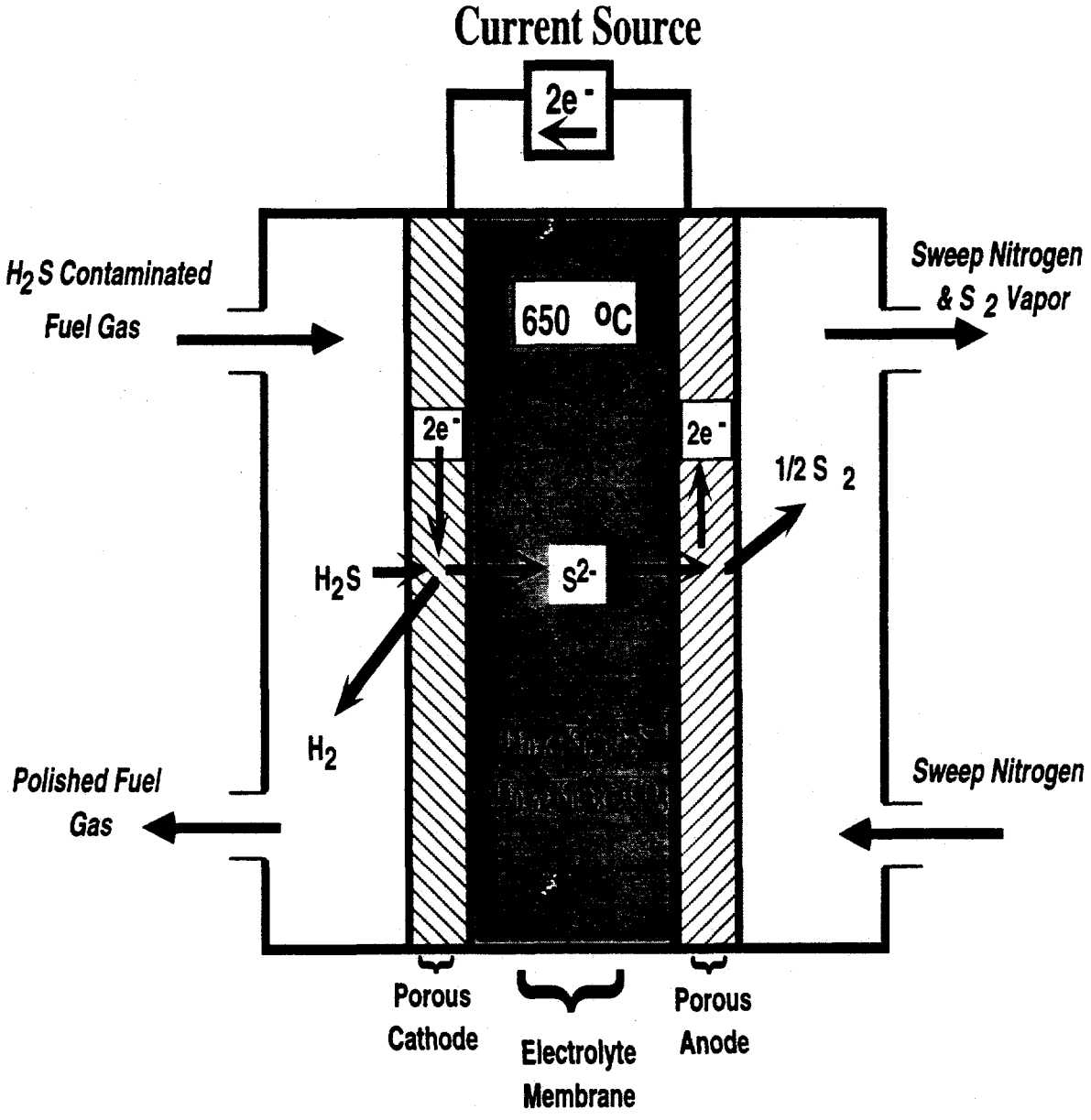

Figure 1. Single-Cell View of the Electrochemical Membrane Separator

Quarterly Summary

Utilizing Ni as a cathode material at reduced temperatures (decrease from 650 ^{o}C to 580 ^{o}C) in full-cell experiments was the primary focus this quarter. A Ni cathode was purchased from ERC and utilized in one full-cell experiments (run 31). The membrane was a fabricated membrane purchased from Zircar Corporation. Table III gives an outline of the membrane materials as well as other components used for experiment 31.

Run 31 served a three-fold purpose: 1) testing the electrochemical membrane separators ability to concentrate CO_2; 2) testing the electrochemical membrane separators ability to remove H_2S; and 3) testing modifications of the experimental apparatus(i.e. Ni cathode performance at 580 C).

Table III. Experimental Components

Run	Temp. ^{o}C	Cathode	Anode	Membrane	Housings	Electrolyte
31	580	Ni	Ni	Fabricated (ZrO_2)	MACOR machineable ceramic	$(Li_{0.62}K_{0.38})_2CO_3$

CO_2 Concentration

Before addition of H_2S to the cell, evaluation of theoretical CO_2 removal from the process-gas (cathode coal syn-gas) **(3)**:

$$CO_2 + H_2O + 2e^- \rightarrow H_2 + CO_3^{2-} \qquad (3)$$

and anode CO_2 evolution **(4)**:

$$CO_3^{2-} \rightarrow CO_2 + 1/2O_2 + 2e^- \quad (4)$$

with applied current was the first test conducted on the Electrochemical Membrane Separator (E.M.S.) full-cell run; percentage of CO_2 removal/evolution compared to the theoretical value, based on 2 Faraday's of charge transferred per mole of species reduced or oxidized, determines system permanence. A current step method was performed in order to determine CO_2 removal, CO_2 evolution, as well as the potential profile at varying currents. CO_2 removal data is given in Figure 2 and cell potentials are illustrated in Figure 3, respectively. H_2S addition to the cell occurred once CO_2 transport performance was proven.

Upon addition of H_2S, cathode gases equilibrated by:

$$H_2 + CO_2 \leftrightarrow H_2O + CO \quad (5)$$

via a stainless steel shift reactor before entering the cell housing. Once process gases entered the cell housings the molten-electrolyte - process-gas equilibrium given by (6)

$$(Li_{0.68}K_{0.32})_2CO_3 + H_2S \Leftrightarrow (Li_{0.68}K_{0.32})_2S + CO_2 + H_2O \quad (6)$$

creates a conversion of carbonate ions to sulfide ions dependent on the partial pressure of H_2S above the electrolyte.

Upon equilibration of the electrolyte and process-gas species (H_2S inlet ~ H_2S outlet at varying flow rates) current was applied to the cell to test H_2S removal capabilities.

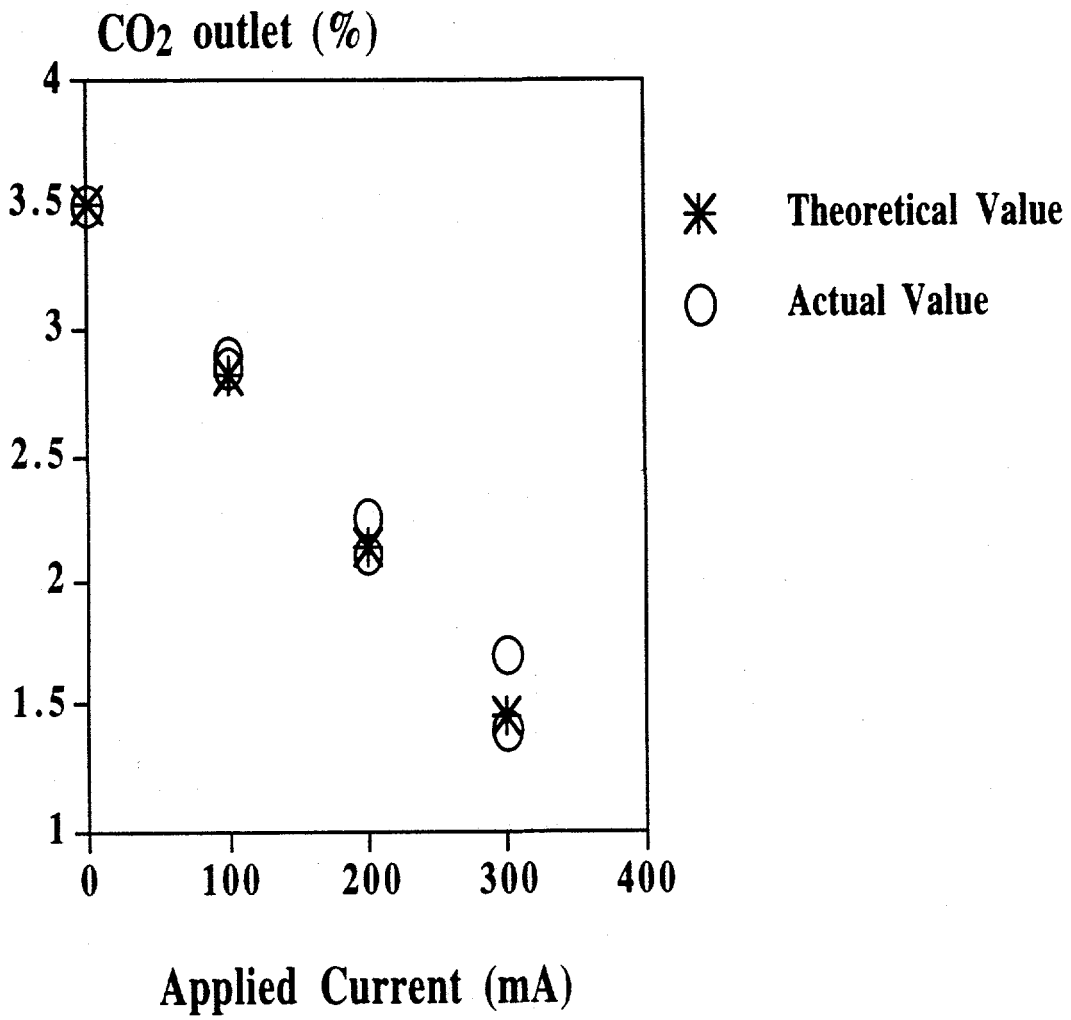

Figure 12. Cathode CO_2 Level vs. Applied Current; Run #31

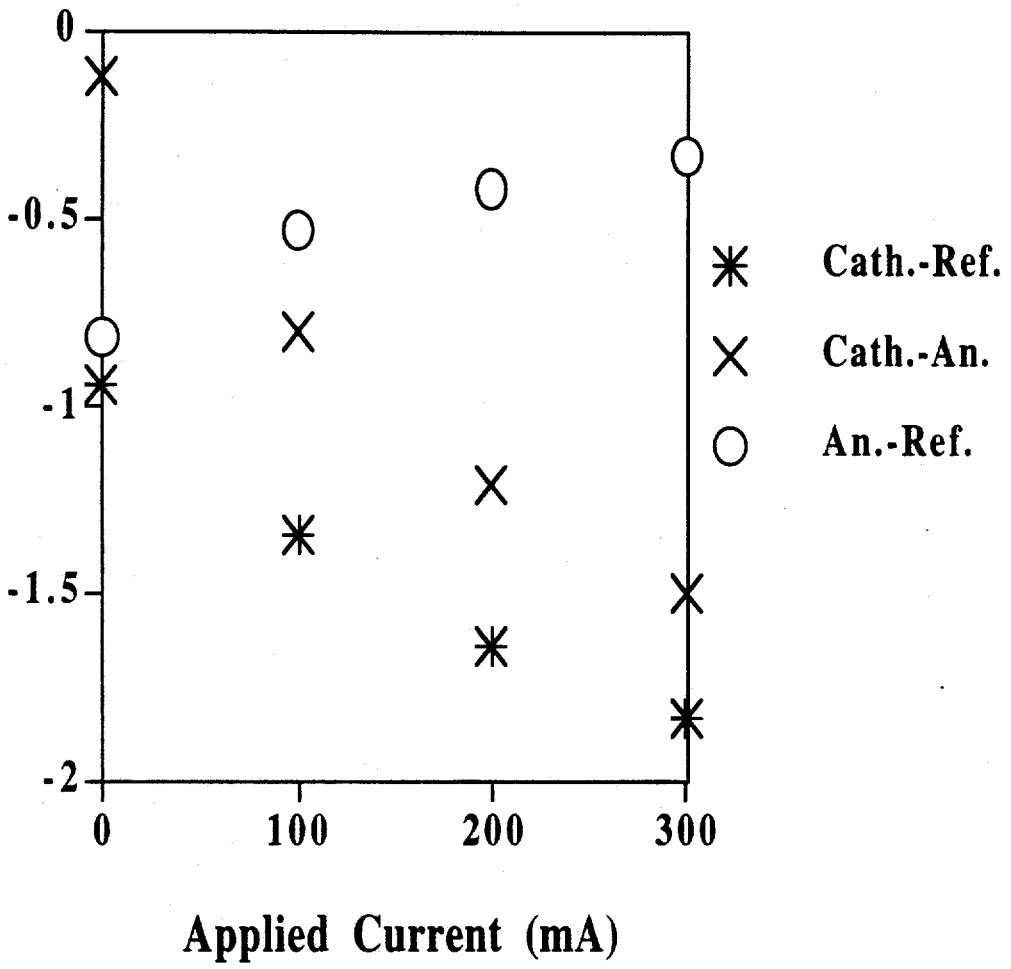

Figure ~~5~~ 3. Run #31 Carbonate Transport: Cell Potential vs. Applied Current

Removal of H_2S from Very Sour Coal Gas

Run #31

Stoichiometric CO_2 removal with current was shown, figure 2; however anodic CO_2 production was limited by sweep-gas seals. Potentials For CO_2 removal across the range of applied current are illustrated in figure 3.

Once system permanence was established through validating CO_2 removal, H_2S was sent to the cell. Process gases equilibrated, at a cathode flow of 265 cc/min, to 5.6% CO_2, 2.2% CO, 8.3% H_2, 6.7% H_2O, and 2500 ppm H_2S. Gas-phase limiting current estimated at 34.24 mA/cm^2 was one-half the membrane limiting current density; electrolyte species were estimated to contain 93.1 mole% $(Li_{0.68}K_{0.32})_2CO_3$ and 6.9 mole% $(Li_{0.68}K_{0.32})_2S$. H_2S outlet versus applied current and $\%H_2S$ removals are shown in figure 4 & figure 5, with over 90% removals from the cathode outlet evidenced. A potential diagram, internal resistance was calculated at 4 Ω, with applied current is given in Figure 6.

Next, flow rate was increased to 440 cc/min (limiting current density in the gas and membrane equals 34.39 mA/cm^2 and 81.77 mA/cm^2) followed by 675 cc/min (limiting current density in the gas and membrane equals 34.46 mA/cm^2 and 104.75 mA/cm^2) maintaining a 2500 ppm H_2S outlet. Internal resistance increased to 5 Ω. Once again 90% H_2S removals were shown, figure 4 and figure 5, along with reasonable potentials, figure 6, with the excessive internal resistance (5 times greater than the normal value of 1 Ω).

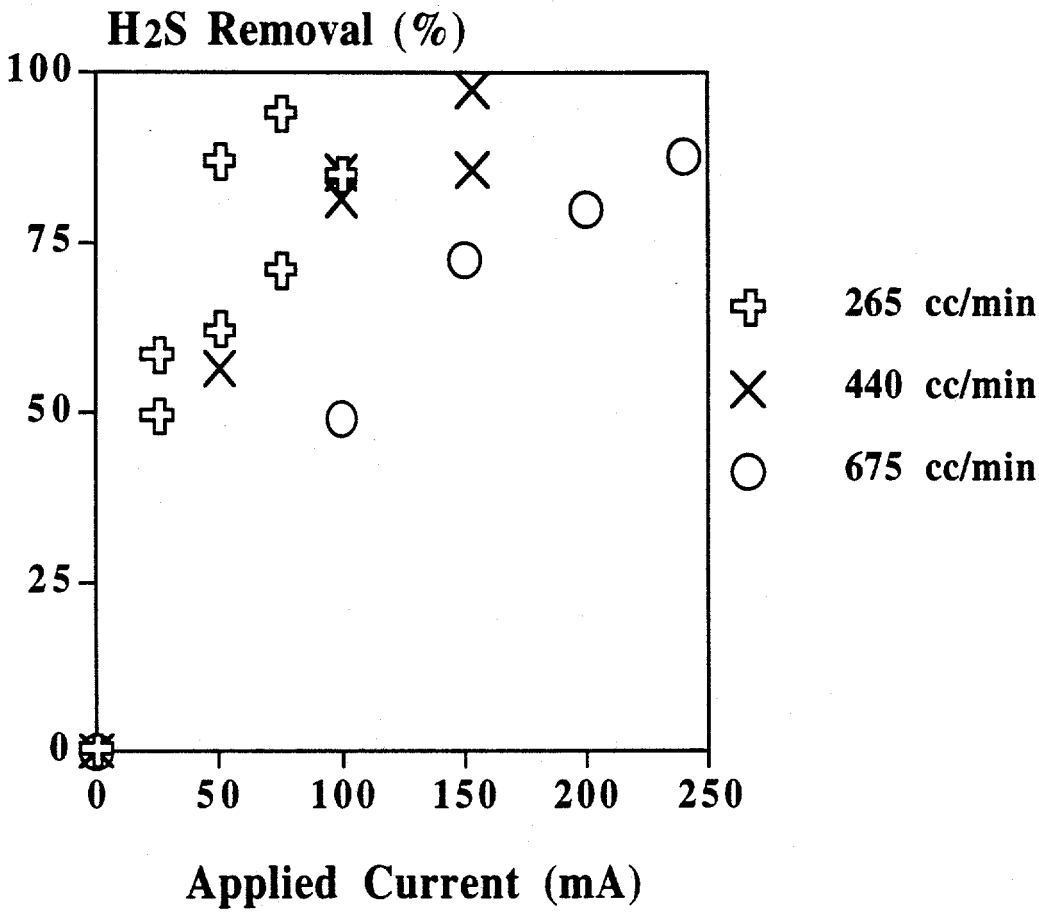

Inlet H_2S: 2500 ppm
Temp.: 580 °C

Figure 4. %H_2S Removal vs. Applied Current; 2500 ppm Inlet H_2S

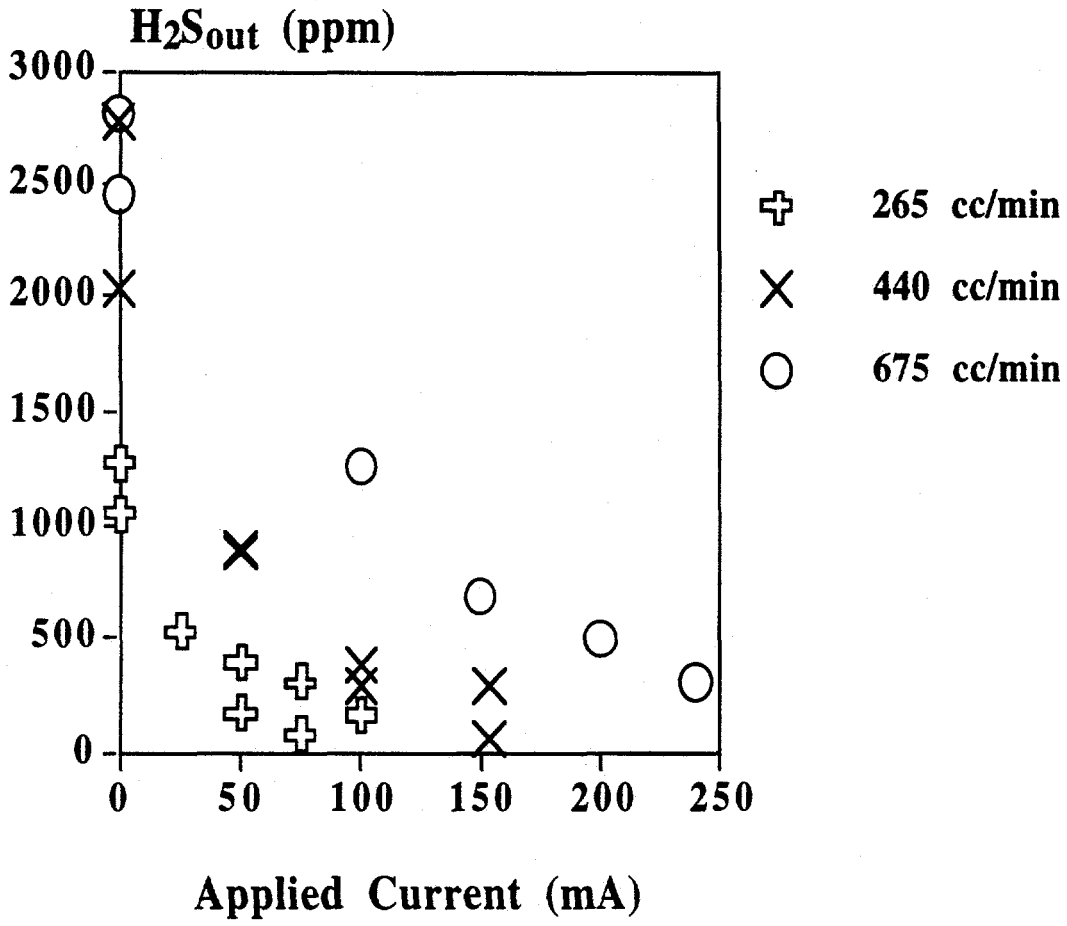

Inlet H_2S: 2500 ppm
Temp.: 580 °C

Figure 5. Outlet H_2S vs. Applied Current; 2500 ppm Inlet H_2S

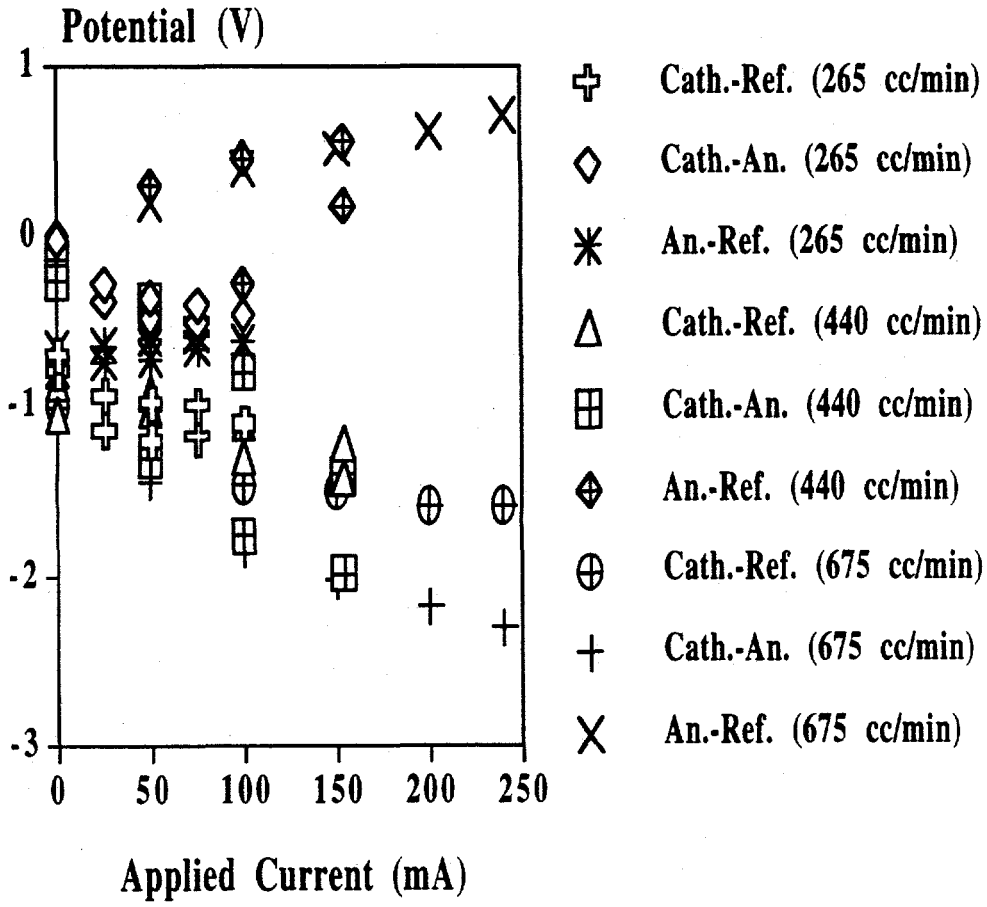

Inlet H_2S: 2500 ppm
Temp.: 580 °C

Figure 6. Cell Potentials vs. Applied Current; 2500 ppm Inlet H_2S

Once effective H_2S removals were shown at 2500 ppm, inlet gas was adjusted with a new inlet value of 4500 ppm H_2S. Gases equilibrated to 12.2% CO_2, 14.5% CO, 21.4% H_2, and 5.6% H_2O creating a calculated electrolyte concentration of 94.4 mole% $(Li_{0.68}K_{0.32})_2CO_3$, 5.6 mole% $(Li_{0.68}K_{0.32})_2S$; limiting current densities were 50.53 mA/cm^2 in the gas-phase and 52.31 mA/cm^2 in the membrane. At these concentrations the cathode flow rate was varied from 130 cc/min to 570 cc/min. 90% removals were shown at varying current in the range of flows, figures 7 & 8. Potentials recorded at different currents, figure 9, were higher than expected but can be explained by the continual loss of electrolyte; internal resistance was around 10 Ω.

Run #31 was eventually shut-down after 408 hours (17 days) due to loss of process-gas seals attributed to the excessive loss of electrolyte.

Post mortem analysis revealed a three-phase change in the cathode from Ni to a combination of $Ni_{3-x}S_2$, NiS (Millerite), and Ni_3S_2 (Heazlewoodite), Figure 10. 0.03 grams of sulfur was recovered from the anode outlet of the cell; verification occurred by heating the powder above its melting point (130 ^oC) creating a viscous-garnet liquid.

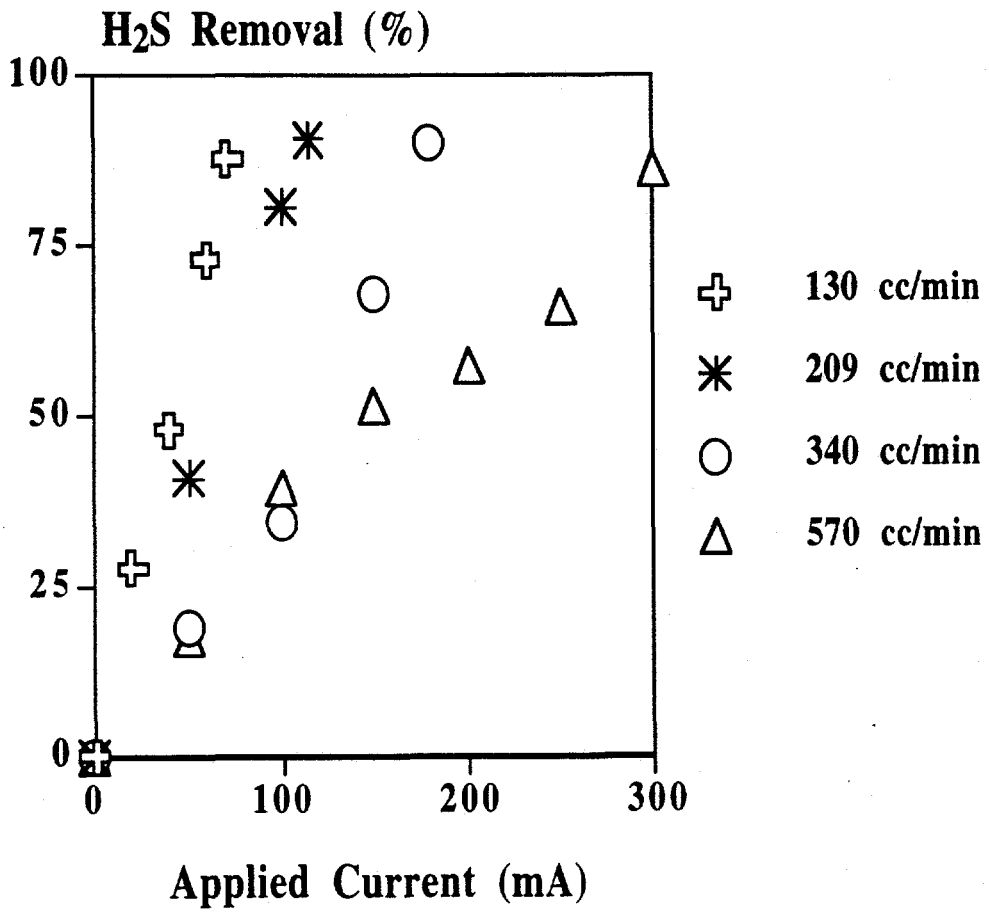

Inlet H_2S: 4500 ppm
Temp.: 580 °C

Figure 7. %H_2S Removal vs. Applied Current; 4500 ppm Inlet H_2S

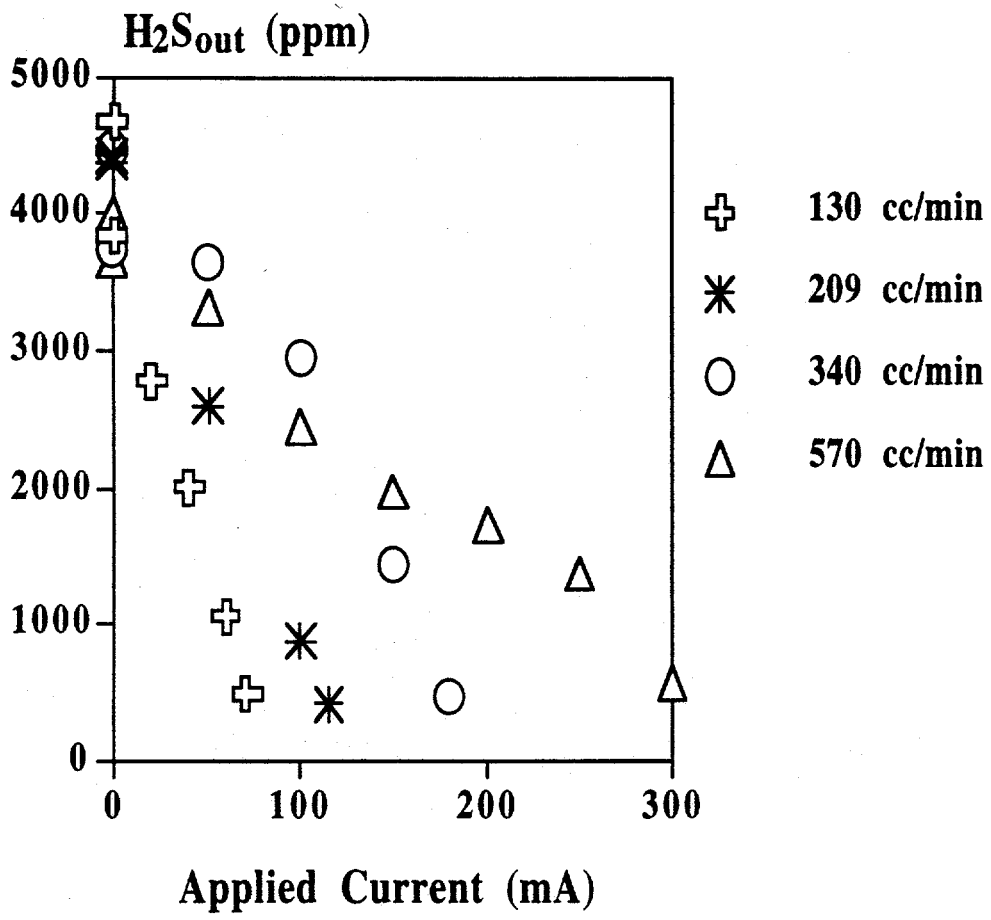

Inlet H_2S: 4500 ppm
Temp.: 580 °C

Figure 8. Outlet H_2S vs. Applied Current; 4500 ppm Inlet H_2S

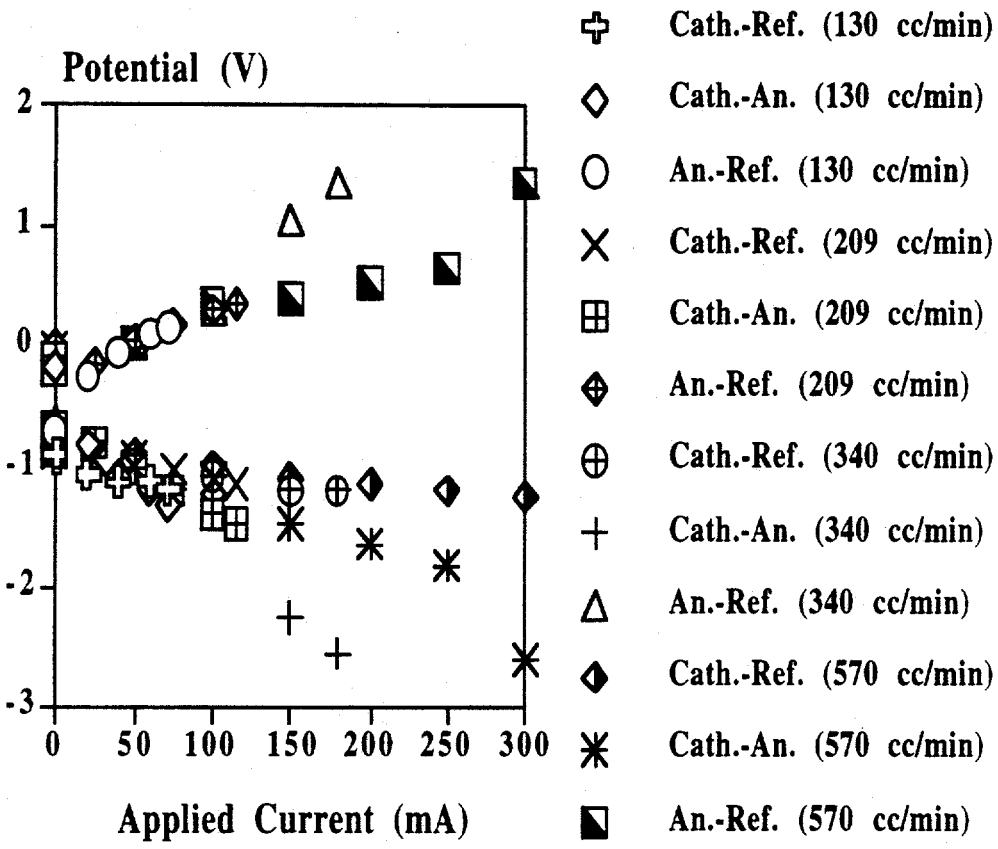

Inlet H_2S: 4500 ppm
Temp.: 580 °C

Figure 9. Cell Potentials vs. Applied Current; 4500 ppm Inlet H_2S

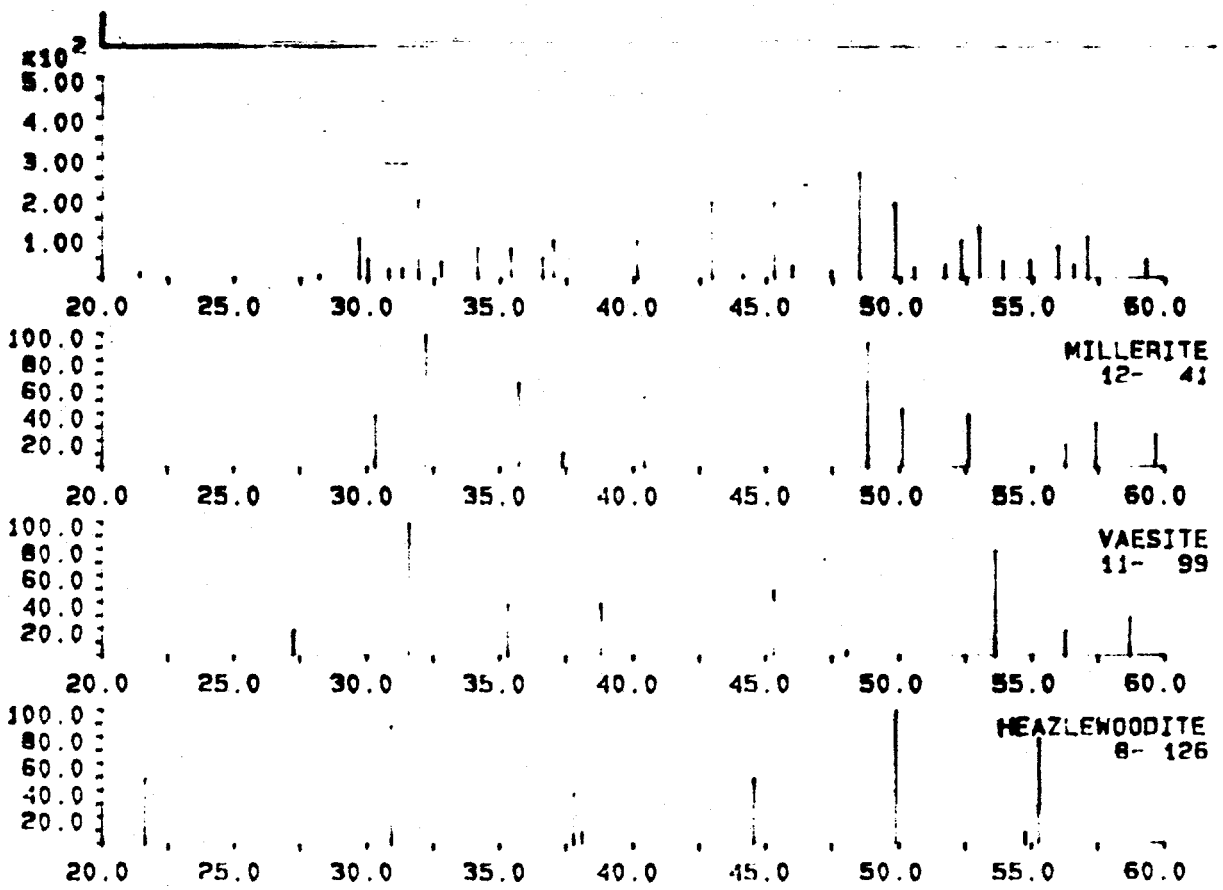

Figure 10. X-ray Diffraction Pattern for Ni Cathode; Run #31

Electrode Materials

Nickel

The nickel-oxygen-sulfur system phase diagram at 580 °C is shown in figure 11; the predominant stable phase in equilibrium with the coal synthesis gas is Ni_3S_2, existing between an H_2S/H_2 ratio of 0.0006 and 0.25. At 650 °C the phase diagram has a small change in these compound windows, figure 12, however the predominant phase remains Ni_3S_2, stable between an H_2S/H_2 ratio of 0.002 and 4.0. This compound

consists of either nickel or sulfur in solid solution with the high temperature form of tetragonal $Ni_{3-x}S_2$; this creates a crystallographic change from hexagonal Heazlewoodite (Ni_3S_2)[14]. This non-quenchable phase exists above 556 °C and separates into the low-temperature form of Ni_3S_2 (Heazlewoodite) upon cooling[14]. Physical property data is rare for $Ni_{3-x}S_2$ and is usually approximated by Ni_3S_2[14,15]. As the H_2S/H_2 ratio of the coal gas stream is lowered, the nickel content in solid solution increases until saturation, at which point a separate nickel phase is formed, figures 11 & 12. A eutectic point for this system is evidenced at 640 °C[14,16] which is well within the operable range of the E.M.S. system, below which operation should be acceptable by maintaining cathode pore morphology; cell operation must be above the electrolyte melting point of 490 °C.

Analysis, by x-ray diffraction, of cathode materials utilized at 650 °C within the $H_2S/H2$ ratio mentioned above revealed the presence of both $Ni_{3-x}S_2$ and Ni_3S_2. Since the cell was operable above the eutectic temperature a common phenomenon evidenced on post-mortem analysis was the cathode diameter on average decreased 25%; this decreased the active surface area by 43%. Current collectors were also embedded within the surface of the cathode. Cathode materials utilized at 580 °C were also analyzed and showed similar phase changes as at 650 °C; however, electrode morphology did not appear to change.

The anode material was in the range of NiO and showed complete chemical and electrochemical stability in full-cell experiment.

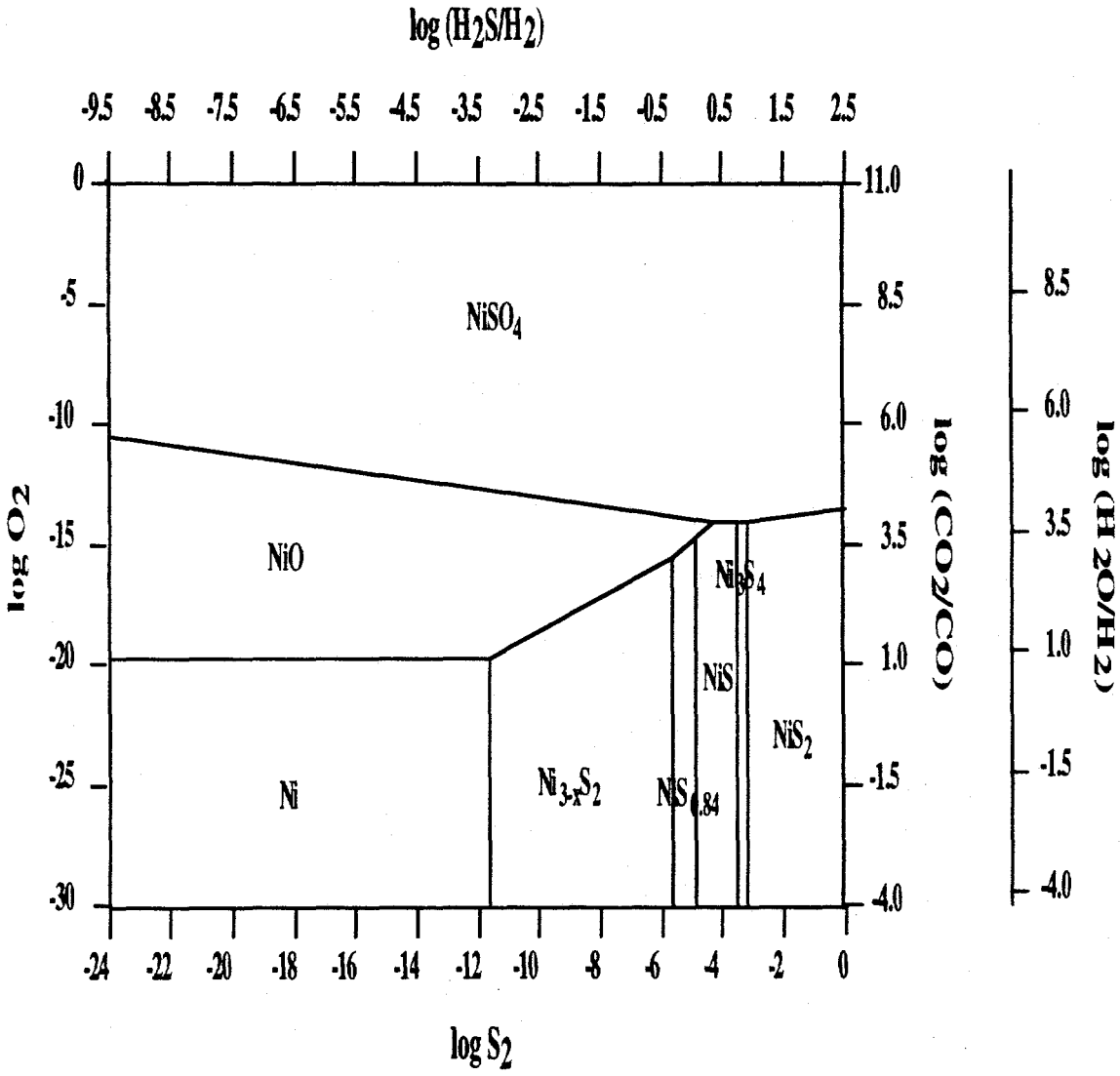

Figure 11. Ni-O-S System Phase Diagram at 580 °C

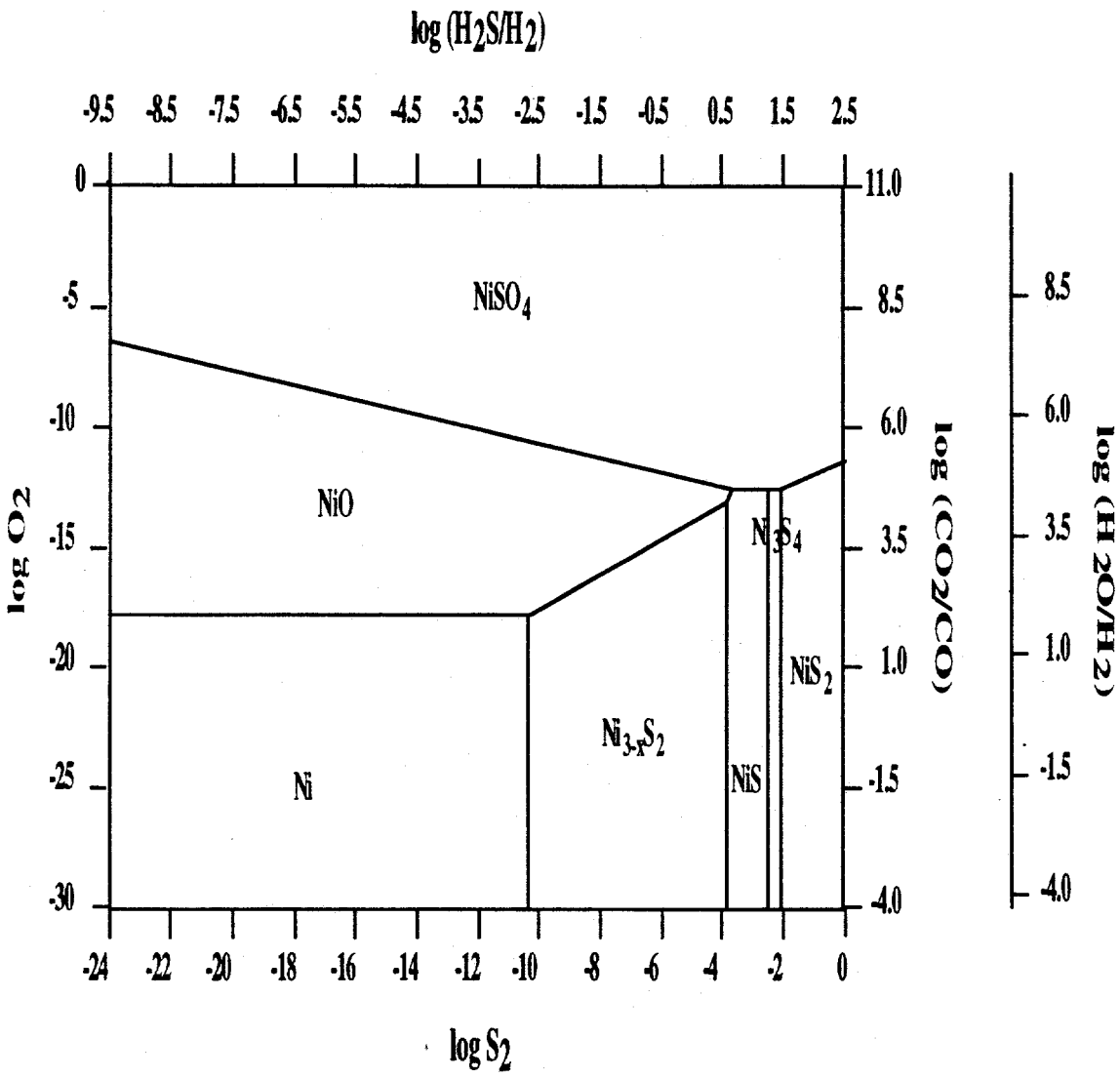

Figure 12. Ni-O-S System Phase Diagram at 650 °C

Discussion

The goal of full-cell experiments was to validate the removal capabilities of the E.M.S. system while maintaining economically viable current efficiencies (high current efficiencies at high inlet H_2S concentrations). H_2S current efficiency is calculated by:

$$\eta_{H_2S} = \frac{\%H_2S\ Removal_{actual}}{\%H_2S\ Removal_{theoretical}} \qquad (7)$$

representing the ratio of H_2S actually removed compared to the theoretical amount that should be removed at a finite applied current.

In this section the current efficiencies and cell potentials of these experiments are compared to those predicted by the theoretical limiting values. This being the prediction of the theoretical limiting H_2S removal performance achievable in the presence of overwhelming levels of H_2O and CO_2 (on the order of 10^5 higher in concentration than H_2S). Predicted current efficiencies and cell potentials were a function of several parameters involved in completing the unit operation including applied current, flow rate, and Nernstian effects. Thermodynamic principles based on standard Gibb's energy and concentration of electro-active species in the gas phase gave the minimum potential requirements in order for cell operation to occur. Upon application of current other factors including electro-kinetics, mass transfer, chemical equilibria, and internal resistance were incorporated into the prediction.

Theoretical predictions, which represent a limiting value, show achievable current efficiencies close to 100 percent for H_2S levels on the order of 1000 ppm at 90% removals. At this same removal level with 100 ppm and 10 ppm inlet gas, the current efficiencies dropped, due to aforementioned concentration effects, to 93% and 40% respectively. This solidifies the importance of obtaining close to 100% current efficiencies at sour gas levels compared to polishing applications where the removal, not the current efficiency, is more important.

Predicted cell potentials were consistently in the same range, -0.450 V to -0.550 V, for all concentration levels at 90% removal.

H_2S current, removal efficiencies, and cell potentials fluctuated over the duration of each experiment. This was mainly attributed to a variation in electrolyte distribution within the system, H_2 permeation, and variable process gas seals. Potentials were IR compensated giving more realistic values.

Experimental error of the collected data (actual values) from the bench-scale apparatus was based on sample collection and analysis equipment not on the changes associated with the aforementioned electrolyte and process seal variabilities; a quantitative value for these variables was not possible. The error is conservatively identified within a 95% confidence interval based on a random sampling distribution of sums and quotients **(7)** & **(8)**.

$$\%H_2S\ \text{Removal} = \frac{\left(\text{Outlet } H_2S_{\text{zero current}} - \text{Outlet } H_2S_{I_{\text{applied}}}\right)}{\left(\text{Outlet } H_2S_{\text{zero current}}\right)} \times 100 \qquad (8)$$

Figure 13 illustrates a successful bench-scale experiment at 580 °C utilizing MACOR housings; current efficiency was within 10% of the theoretical maximum value at 90% removals. Ni cathode morphology remained constant throughout the duration of the experiment converting to Ni_3S_2 without incurring the phase transition associated with $Ni_{3-x}S_2$.

Potentials, shown in figure 14, were higher than those predicted by the model due mainly to a high internal resistance (4 times greater than the standard value of 1 ohm) dampening ionic mobility. The compensated potentials are also given, showing an increase in potential with $\%H_2S$ removal; this was again attributed to increasing H_2 permeation through the membrane.

A yellow solid, 0.03 grams of sulfur, was collected from the anode outlet tube. The calculated amount based on applied current, current efficiency, and time was 1 gram. The reason for the low sulfur yield was attributed to losses through incomplete condensation of the vapor on the inside of the

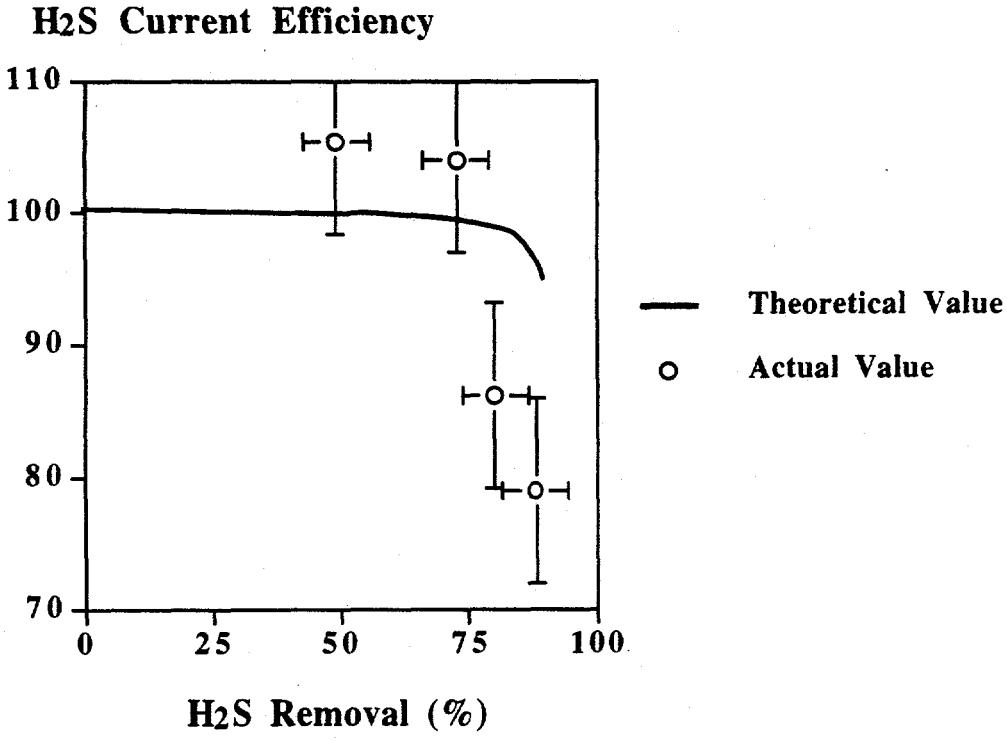

Inlet H_2S: 2500 ppm
Temp.: 580 °C
Cathode Flow: 675 cc/min

Figure 13. Comparison of Theoretical and Actual Values; %H_2S Removal vs Current Efficiency for Run #31

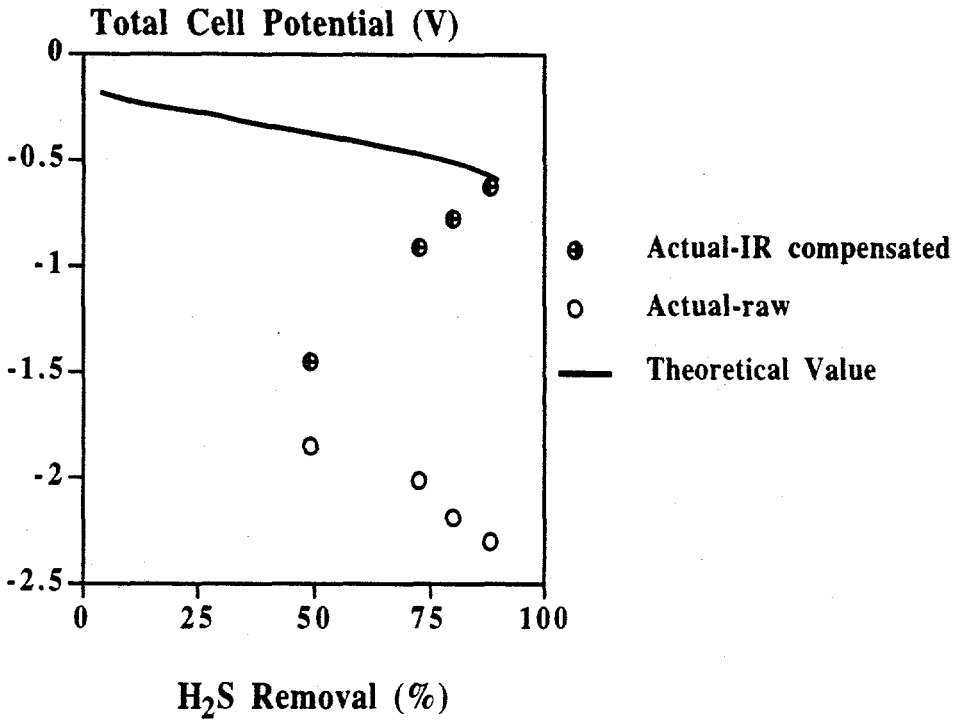

Inlet H_2S: 2500 ppm
Temp.: 580 °C
Cathode Flow: 675 cc/min

Figure 14. Cell Potentials vs %H_2S Removal; Theoretical vs Actual Values for Run #31

anode outlet tube (some particulates escaped through the outlet tube). Other losses were associated with faulty process gas seals. Nevertheless, this was the first positive sign at the anode side of the E.M.S system of sulfur liberation (2) taking precedence over the competing parasitic reaction (4).

$$S^{2-} \rightarrow 1/2S_2 + 2e^- \qquad (2)$$

$$CO_3^{2-} \rightarrow CO_2 + 1/2O_2 + 2e^- \qquad (4)$$

Since H_2S is the lone source of sulfur entering the cell, reaction (2) validates sulfur liberation at the anode, as well as reaction (6),

$$(Li_{0.62}K_{0.38})_2CO_3 + H_2S \leftrightarrow (Li_{0.62}K_{0.38})_2S + CO_2 + H_2O \qquad (6)$$

providing the necessary ionic pathway for sulfide transport.

Past vs. Present

Past experimentation on the E.M.S. system at varying levels of inlet H_2S has demonstrated high removal capabilities, but at relatively low current efficiencies. Figure 15 represents one of the best results obtained from previous bench-scale experiments.

Removals and current efficiencies were increased ~20% when operating the system at 580 ^oC, with Ni electrodes, at sour gas concentrations. Comparison with the sour gas experiment, illustrated in Figure 15, revealed higher current efficiencies although electrode & membrane materials differed. Improvements in both areas have drastically improved not only removal results but assembly and effective long-term operation of the bench-scale apparatus.

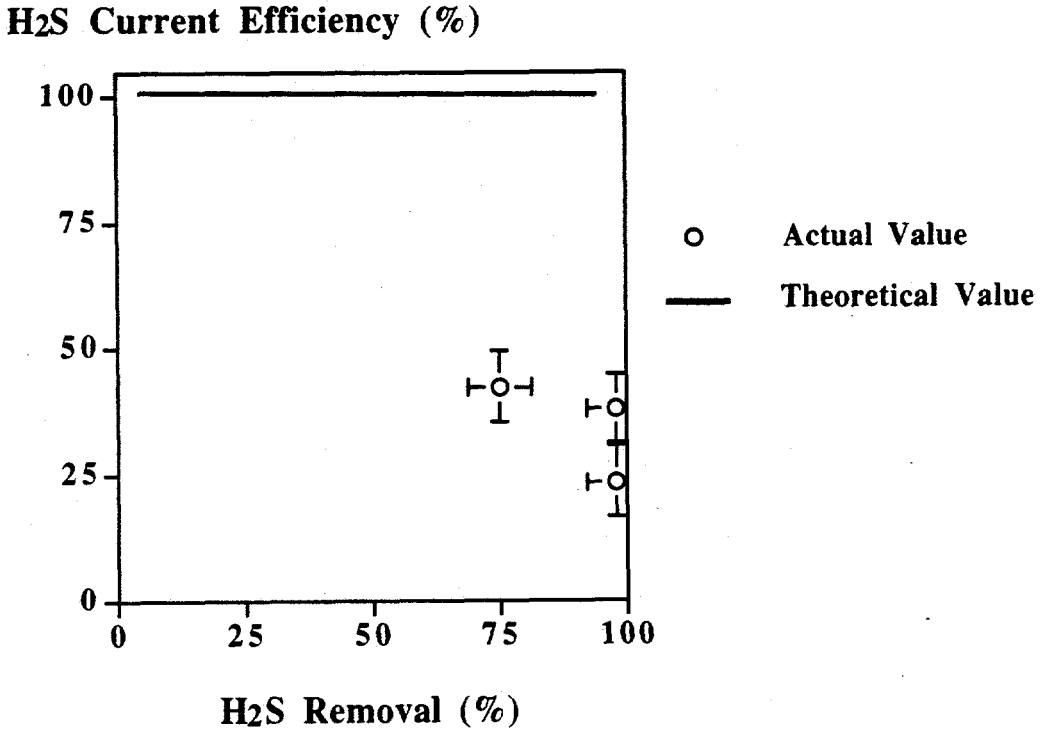

Inlet H_2S: 13000 ppm
Temp.: 650 oC
Cathode Flow: 75 cc/min

Figure 15. %H_2S Removal and Current Efficiency Collected by Weaver[17] Compared to the Theoretical Model Prediction

Conclusion

The Fossil Energy Advanced Research Program requires high temperature separations to remove environmental contaminants from post-combustion flue gases as well as pre-combustion process gases. This project is aimed at the latter: the removal of hydrogen sulfide from coal gas at gasifier temperatures. This development would enable a simplification of the entire gasification scheme by permitting a one-step removal of hydrogen sulfide and production of elemental sulfur. Energy savings accrue due to the high temperature processing.

The DOE programs relating to gasification for power production have as their goal the more efficient, clean paths toward affordable energy from coal. Gas clean-up accounts for nearly one-third of the cost of this conversion. Simplification and economization will benefit the entire effort.

Project Output

Current experiments are based on improving selective removal from initial H_2S concentrations ranging from contaminant levels to very sour levels. High flow rate effects, membrane stability and selectivity, and electrode morphology characterizes present studies, with recent results showing over 90% H_2S removal with applied current.

Contaminant Level Removals

Two experiments have demonstrated the polishing application of the E.M.S. system. In the first, outlet H_2S levels were reduced from 10 ppm to ~1 ppm or 90% removal. The current efficiency at this removal level was 12.6% which compared favorably to the theoretical model prediction of 30.8% current efficiency at 90% removal. H_2S current and removal efficiencies are illustrated in figure 16. Potentials at 90% removals were ~ -0.012 V (the theoretical value is -0.521 V, figure 17). The discrepancy in actual vs predicted potentials can be explained by H_2

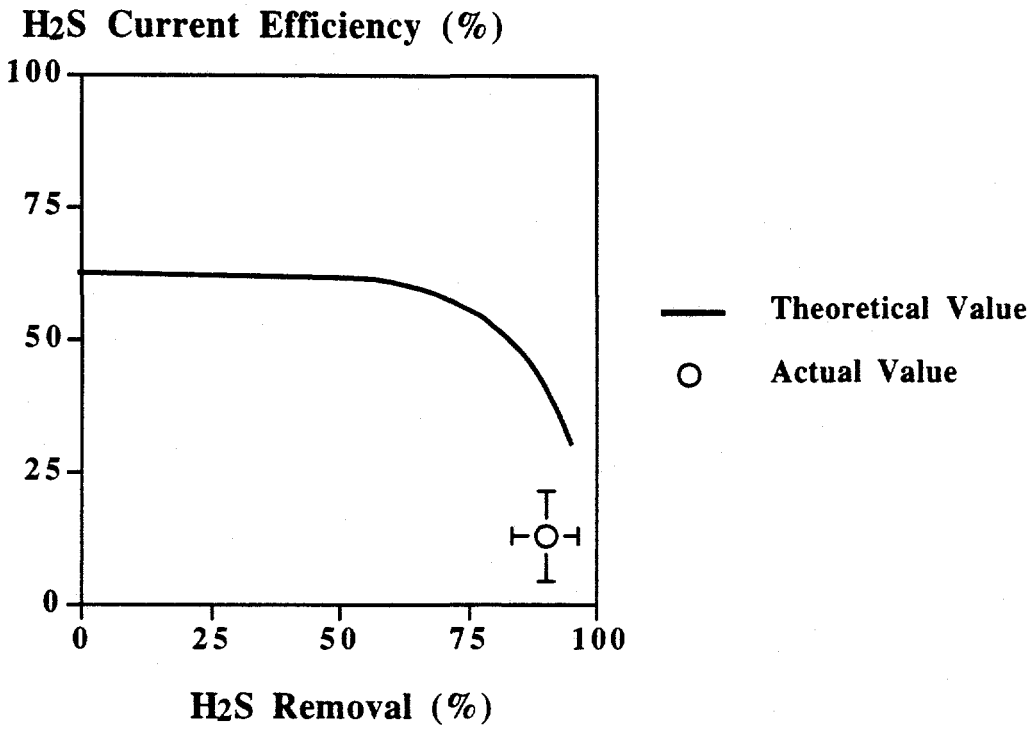

Inlet H_2S: 14 ppm
Temp.: 650 °C
Cathode Flow: 215 cc/min

Figure 16. Comparison of Theoretical and Actual Values; %H_2S Removal vs Current Efficiency

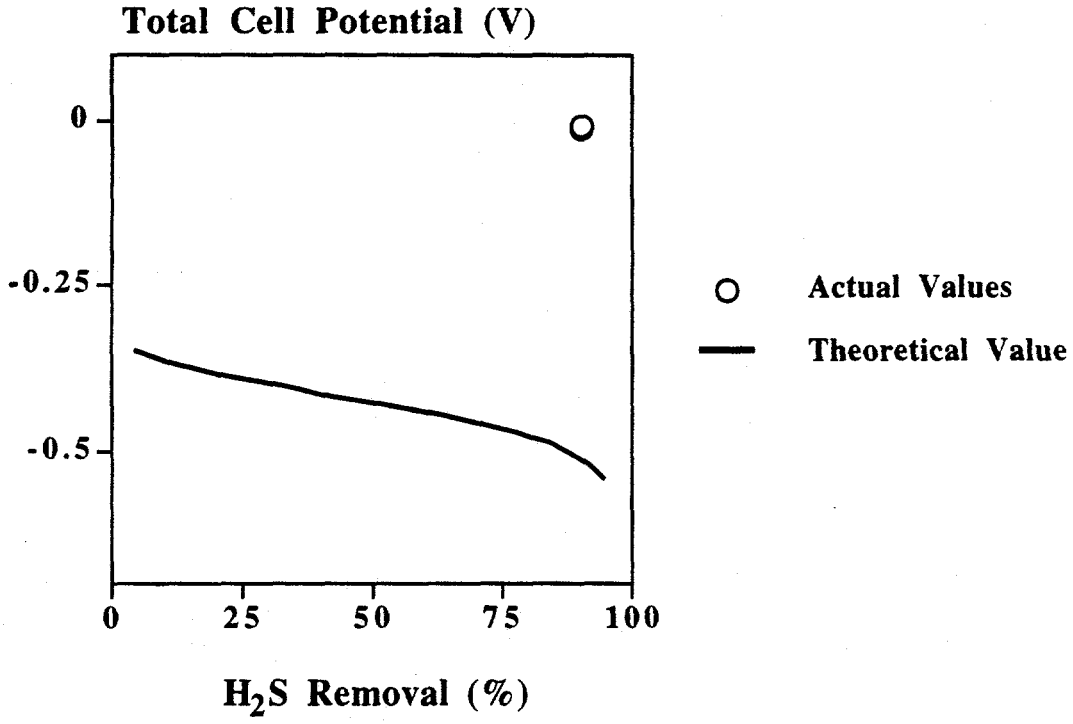

Inlet H_2S: 14 ppm
Temp.: 650 oC
Cathode Flow: 215 cc/min

Figure 17. Cell Potentials vs %H_2S Removal; Theoretical vs Actual Values

cross-over, detailed earlier, associated with electrolyte loss from MACOR degradation. The Ni cathode also remained chemically stable (no conversion to Ni_3S_2 or the eutectic $Ni_{3-x}S_2$) at these removal levels.

In the second, polishing of H_2S from a contaminant gas was accomplished utilizing a purchased zirconia membrane. Over 80% removals occurred at varying flow rates. Electrodes donated from ERC remained stable throughout the duration of the experiment; no morphology change associated with the phase transition to Ni_3S_2 occurred due to the low levels of H_2S in the cathode gas. Bench-scale current efficiencies (50% at 80% removals) agreed well with the theoretical predictions (68% at 80% removals) in a similar relationship to those of run 21 (~20% below the theoretical maximum value). However, fluctuation occurred over the experimental run, due in part to a change in flow rate and electrolyte loss associated with the MACOR housings (IR varied from 1 to 3 ohms). Figure 18 and figure 19 illustrate the removals of H_2S from the cathode gas. Figure 18 gives a representative proximity of the theoretical values to bench-scale data at a cathode flow of 375 cc/min. Actual potentials were much less than those predicted, illustrated in figure 19, due to H_2 cross-over.

H_2S Removals From Very Sour Coal Gas

Successful application of the E.M.S. technology to sour coal gas is shown in figure 20. The H_2S current and removal efficiencies demonstrate the actual bench-scale values agreement with the model predictions; current efficiencies were within 10% of the maximum theoretical values. Applied current exceeded the stoichiometric value at 90% H_2S removal (from 1700 ppm to 141 ppm) by 45 mA. Potentials remained low (~0.100 V below theoretical value shown in figure 21, representing compensated and uncompensated values) which is economically beneficial at this level of H_2S removal; MACOR degradation created a deficiency of electrolyte allowing a pathway for H_2 cross-over.

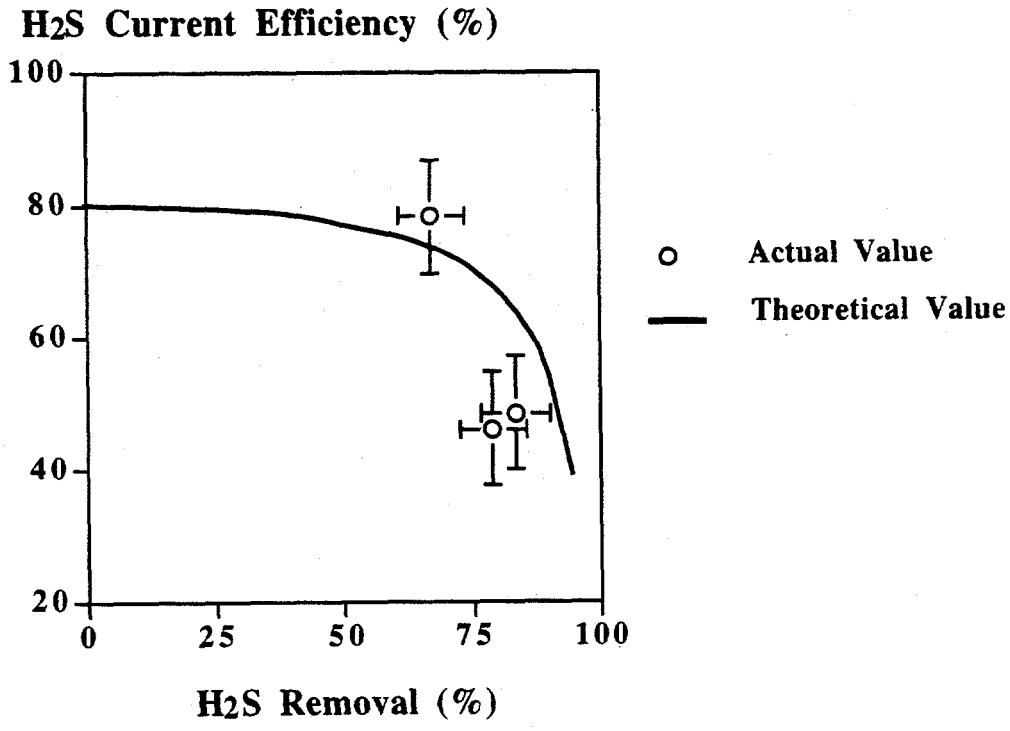

Inlet H_2S: 25 ppm
Temp.: 650 oC
Cathode Flow: 375 cc/min

Figure 18. Comparison of Theoretical and Actual Values; %H_2S Removal vs Current Efficiency

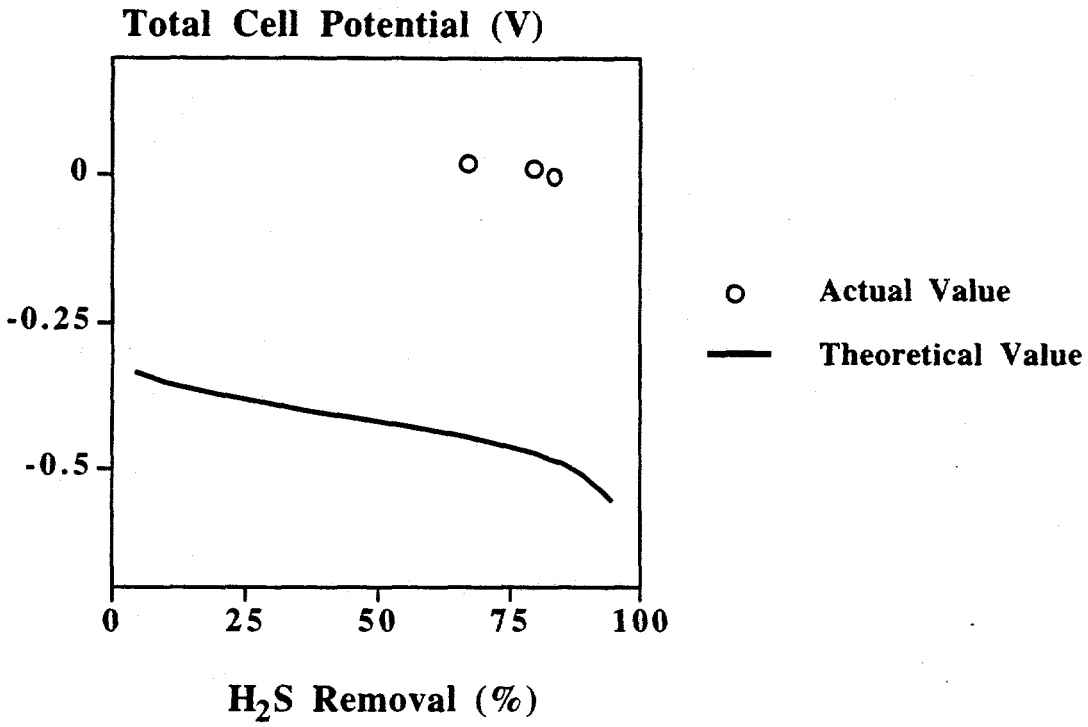

Inlet H_2S: 25 ppm
Temp.: 650 oC
Cathode Flow: 375 cc/min

Figure 19. Cell Potentials vs %H_2S Removal; Theoretical vs Actual Values

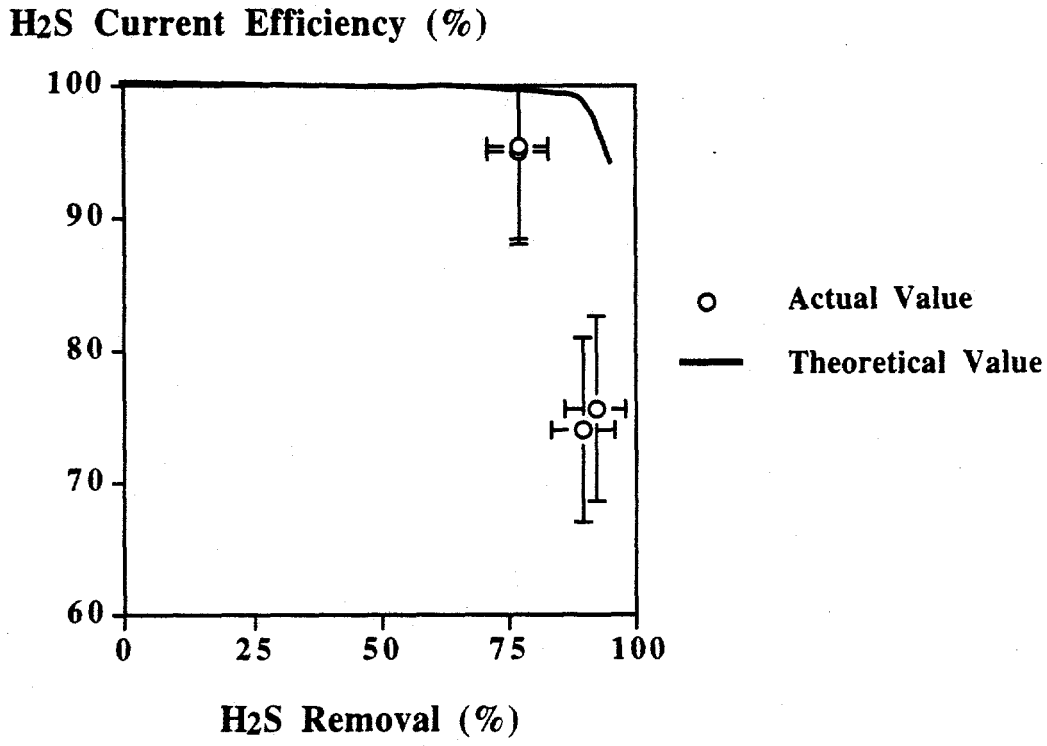

Inlet H_2S: 1630 ppm
Temp.: 580 oC
Cathode Flow: 560 cc/min

Figure 20. Comparison of Theoretical and Actual Values; %H_2S Removal vs Current Efficiency

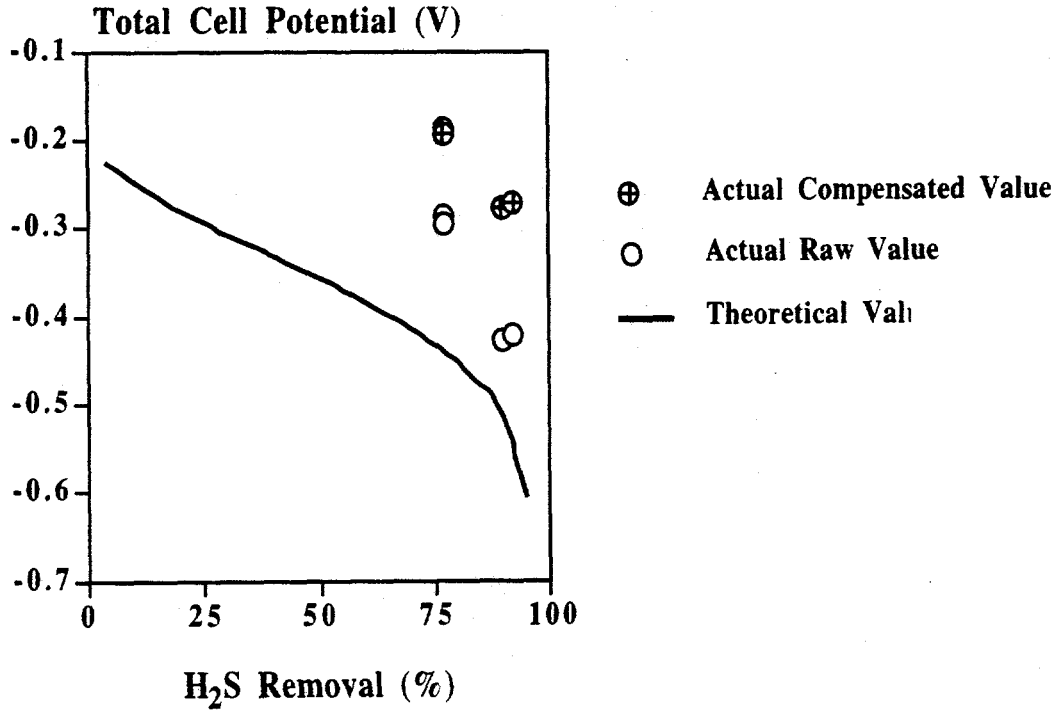

Inlet H_2S: 1630 ppm
Temp.: 580 °C
Cathode Flow: 560 cc/min

Figure 21. Cell Potentials vs %H_2S Removal; Theoretical vs Actual Values

Since the cell was operated at 580 ^{o}C, 70 ^{o}C below polishing operation temperature, the Ni cathode converted to the predicted compound, Ni_3S_2; no evidence of the eutectic phase $Ni_{3-x}S_2$ was identified since the cathode morphology remained constant and current efficiencies were realistic for scale-up application.

Next Quarter Goals

A continual problem with the E.M.S. system is an appropriate cathode material with chemical and electrochemical stability in the high temperature corrosive environment. At high levels of H_2S, the Ni cathode converts to a molten NiS_y creating adverse effects mentioned previously. A review of the literature[21] revealed that maintaining a temperature below 635 C, usual experiments are performed at 650 C, prevents the liquid NiS_y from forming. Next quarters experiments will be performed at 600 C with the E.R.C. Ni electrodes at the anode and the cathode. Co electrodes will continue to be investigated as well; however, persistent oxidation of the material during binder-burn-out has created adverse reactions schemes upon applications of current exposing permanent damage to E.M.S. system.

Stainless steel housing materials will also be the focus of future work since a less exotic material, other than MACOR, is necessary for eventual scale-up.

References

1. U.S. Dept of Energy, DOE/METC 87/0255, DE87006493, Oct., 1987.
2. Skerret, P.J., "Fuel Cell Update", *Popular Science*, 89-91, 120-1, June, 1993.
3. Lim, H.S. and Winnick, J., *J. Electrochem. Soc.*, **131, 562-8** (1984).
4. Alexander, S., and Winnick, J., *1990 AIcHE Annual Meeting*, Chicago, IL., 1990.
5. Alexander, S., and Winnick, J., *Sep'n Sci. and Tech.*, **25**, 2057-72 (1990).
6. Weaver, D., and Winnick, J., *J. Electrochem. Soc.*, **134**, 2451-58 (1987).
7. Weaver, D., and Winnick, J., *J. Electrochem. Soc.*, **138**, 1626-37 (1991).
8. Banks, E., and Winnick, J., *J. Appl. Electrochem.*, **16**, 583-90 (1986).
9. White, K.A., and Winnick, J., *Electrochim. Acta*, **30**, 511-516 (1985).
10. EPRIEM-1333, *Assessment of Sulfur Removal Processes for Advanced Fuel Cell Systems, Final Report,* C.F. Braun and Co., Alhambra, CA, Jan., 1980.
11. Vidt, E.J., DOE/METC DE-AC-21-81MC16220, DE82013942, Westinghouse, Dec., 1981.
12. Focht, G.D. et. al., DOE/MC/121166-2163, DE86016041, July, 1986.
13. Lyke, S.E., DOE/MC/19077-1803, DE8500961, Battelle Pacific Northwestern Laboratories, Jan. 1985.
14. Kullerud, G. and Yund, R.A., *J. of Petrology*, **3**(1), 1962.
15. Rosenquist, T., *J. of the Iron and Steel Institute*, Jan. 1954.
16. Niu, Y., Viani, F., and Gesmundo, F., *Corrosion Science*, **36**(5), 1994.
17. Weaver, D., and Winnick, J., *J. Electrochem. Soc.*, **139**, 492-498 (1992).